International Journal of Concrete Structures and Materials

RESEARCH Open Access

# Evaluating Grid Frame-Type Railroad Derailment Containment Provisions with Drop Weight Impact Testing

Yun-Suk Kang[1*], Hyun-Ung Bae[2], Tae-Hoon Kim[1], Choon-Seok Bang[1], Nam-Hyung Lim[3], Chan-Young Lee[4] and Woo-Jin Han[5]

## Abstract

This study evaluates the structural performance of newly designed and fabricated grid frame-type railroad DCPs (derailment containment provisions) classified as DCP type I, compatible with rapid assembly construction and maintenance on gravel tracks in railway service lines. Previous research only reviewed the durability of the structure under static loading conditions. However, this study proposed an evaluation method considering the importance of assessing the impact performance of the DCPs assembly structure subjected to dynamic impact loads from continuously colliding train wheels; this involved a drop weight test to analyze the behavior of the DCP assembly structure under accumulated impact energy applied to different collision positions. To this end, drop-impact weight tests were conducted to verify the structural performance of the derailment protection system connected to concrete sleepers using post-installed anchors. A test specimen and jig were fabricated to evaluate the structural performance and impact resistance of the anchoring connections. 15 drop weight impact tests were performed, and the resulting behavior under impact energy was analyzed.

The results indicated that when a derailed train wheel collides with the DCP frame section, dominant loads act on the base plate anchor, resisting through shear and bearing strength of the anchor bolts. The DCP assembly structure demonstrated sufficient derailment containment performance, even under significant accumulated energy (21.0 kJ; six repeated impacts), with collision loads and displacement levels within acceptable limits. For repeated impact loads (3.5~7.0 kJ; 1~2 occurrences), the impact load absorbed by the DCP connection anchor averaged 241.22 kN, and the vertical displacement at the collision point averaged 14.23 mm. This value is 2.62 times (162%) greater compared to the case of a collision on the DCP frame and approximately 13% lower than the impact load that the DCP frame can absorb. Additionally, when a derailed wheel collided directly with the side of the base plate, the embedded anchors in the sleeper were identified as a relatively weak point. Therefore, reducing the base plate width (from 500 mm to 480 mm) to guide collisions toward the DCP frame section, which could absorb greater impact loads, was a more effective design. The test results demonstrated that the newly developed steel grid frame-type DCP combination structure sufficiently resists the impact loads from derailed wheels of high-speed trains traveling at 300 km/h. It effectively restricts excessive lateral movement of derailed trains and provides guiding capability. Furthermore, the drop weight test for the newly proposed DCP combination structure, which also considers impact energy, is deemed more suitable for analysis than conventional testing methods.

**Keywords** DCP, Derailment, Containment, Provisions, Structural performance, Derailed wheel, Grid frame, Anchor

*Correspondence:
Yun-Suk Kang
yskang@krri.re.kr
Full list of author information is available at the end of the article

## 1 Introduction

While train derailments and collisions are rare in railway operations, they can cause significant damage, highlighting the need for systematic management by railway organizations. Recently, there have been global accident instances caused by train derailments (FRA, 2011; Iwnicki et al., 2006). In South Korea, between 2013 and 2022, derailments accounted for 51 of the 68 railway accidents, comprising 75% of the total, causing considerable damage (Aviation & Railway Accident Investigation Board, 2023).

Over the past several decades, significant technological advancements have been made in the field of protective systems to address these issues. While preventing accidents altogether is ideal, damage caused by human error, earthquakes, strong winds, track buckling, and wheel defects is unavoidable. To minimize the damage after a derailment, three types of derailment containment provisions (DCP) have been developed and implemented in railway operations to date (Bae, 2015; Bae & Lim, 2024; Bae et al., 2018a, 2018b; Liu et al., 2012, 2017; Wu et al., 2014).

This technology aims to reduce excessive lateral movements and collision accelerations of derailed trains following the primary damage to the vehicle and track; this minimizes secondary damage, such as derailments causing trains to fall from bridges or collide with overhead bridges and adjacent structures. As illustrated in Fig. 1, DCPs are classified into three types (Bae & Lim, 2024; Hamilton & Inc., 2004):

- DCP Type 1: installed within the track gauge to collide with derailed wheels.
- DCP Type 2: installed outside the track gauge to collide with derailed wheels.
- DCP Type 3: installed outside the track gauge to collide with the axle and bogie of the derailed train.

Among DCP Type 1 designs, guardrails on bridges, as illustrated in the top-right side of Fig. 1a, are traditional derailment containment structures. These guardrails are installed parallel to the main running rails within the gauge on sleepers to control the trajectory of derailed trains. They ensure that derailed wheels remain within the bridge deck, protecting girders and other

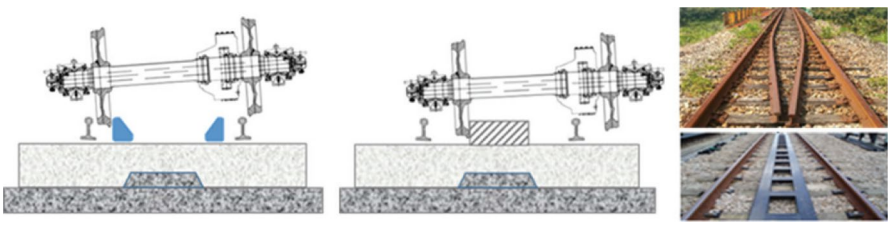

(a) DCP Type 1

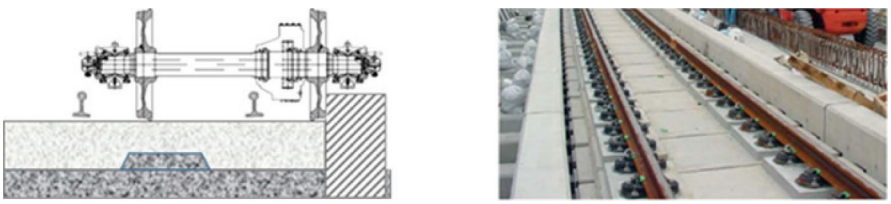

(b) DCP Type 2

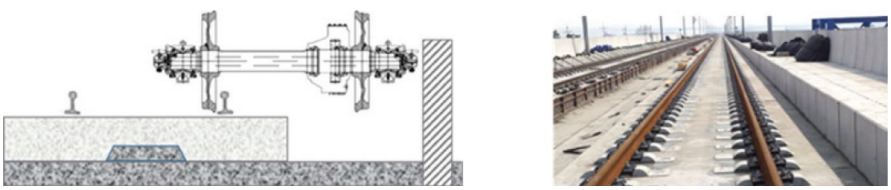

(c) DCP Type 3

**Fig. 1** Types of derailment containment provisions (DCP) (Massachusetts Board of Railroad Commissioners, 1888)

components, thereby reducing impact forces and guiding derailed trains safely across the bridge (Massachusetts Board of Railroad Commissioners, 1888).

In DCP Type 3 designs, protective walls on bridges, as shown in Fig. 2, are installed on the sides of bridge superstructures. The inner wheels are first guided by the outer rails before the train body impacts the wall (robust kerb), ensuring that the derailed train remains within a designated track area and preventing it from falling off the bridge (Railtrack PLC (Safety and Standards Directorate), 2000).

The height of the protective wall is designed to exceed 350 mm from the rail top, with a clearance distance of 1500 mm from the running edge of the rail. The design load considers a lateral force of 100 kN due to train hunting motions. Unlike DCP Type 1 guardrails, which only control the trajectory of the derailed wheels, DCP Type 3 protective walls also provide impact resistance for greater collision loads, guiding both wheels and train bodies (Network American Association of State Highway & Transportation Officials, 2007; Rail, 2011).

Among DCP Type 1 designs, concrete plinths, as illustrated in Fig. 3, are installed on Rheda concrete track (Hamilton & Inc, 2004). During the initial track construction of the Netherlands' HSL-Zuid high-speed rail (2004), concrete plinths were cast in place and cured for 28 days. These DCPs, located at the center of the track, minimized the lateral movement of derailed trains and reduced impact energy. Unlike side-mounted protective structures, these single-structure DCPs improved both safety and cost-effectiveness, making them suitable for high-speed rail operations at speeds of up to 300 km/h.

Subsequently, precast panel-type DCPs for DCP Type 1 were developed for rapid installation on concrete tracks, as illustrated in Fig. 4. This panel is a prefabricated precast panel with a width of 400 mm, a height of 200 mm, and a length of 1.95 to 2.28 m, capable of ensuring protective performance during a derailment at 300 km/h on a high-speed railway curve with a radius of R = 3500 m (Korea Agency for Infrastructure Technology Advancement (KAIA), 2020). These panels resisted derailment impact loads of up to 114 kN on straight tracks and 165.6 kN on curved tracks, withstanding impact energy of 3.3 kJ. Consequently, unlike conventional DCP Type 1, which required cast-in-place construction at the track site, the newly developed system allows prefabricated panels to be produced in factories, anchored to existing operational concrete tracks, and attached to the track surface for rapid on-site assembly. Traditional concrete track plinths could only be installed on newly constructed tracks due to the prolonged train operation suspension required during the concrete curing period. Conversely, the newly developed DCP enables high-quality rapid installation and post-derailment track restoration within a limited downtime (e.g., within a 3-h overnight maintenance window) on existing railway lines that previously lacked derailment containment provisions (DCP) (Korea Agency for Infrastructure Technology Advancement (KAIA), 2020). Furthermore, as illustrated in Fig. 4, the DCP installed at the center of the track guides derailed wheels using the precast panels, preventing the derailed train from deviating significantly from the track.

**Fig. 3** Cast-in-place concrete plinth on Rheda concrete track (Hamilton & Inc, 2004)

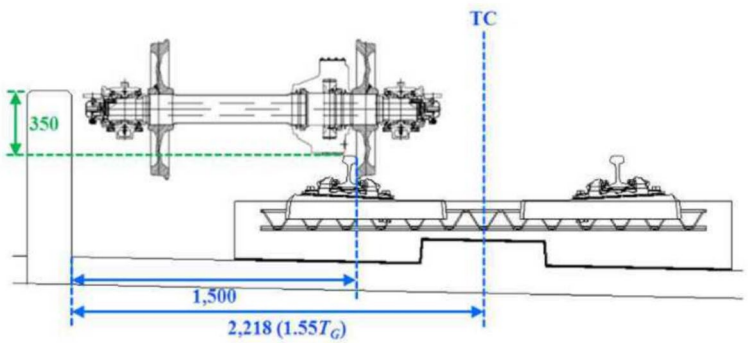


**Fig. 2** DCP concept of robust kerbs on railway bridge (DCP Type 3) (Railtrack and (Safety Standards Directorate) 2000)

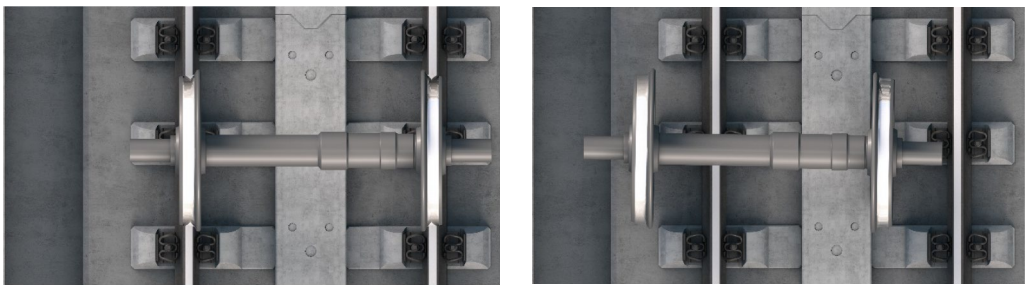

(a) Wheel Set before Derailment (b) Wheel Set after Derailment

**Fig. 4** DCP (derailment containment provision) conceptual diagram (Korea Agency for Infrastructure Technology Advancement (KAIA), 2020)

**Fig. 5** Concrete panel-type DCP of ballasted track (DCP Type 1)

**Fig. 6** Steel frame grid type DCP of ballasted track (DCP Type 1)

Subsequently, among the types of DCP Type 1, a concrete panel-type DCP and a steel frame-type DCP capable of rapid installation on ballasted tracks were developed, as illustrated in Figs. 5 and 6. Given the absence of established standards and systematic guidelines in Korea for the design loads, installation locations, and specifications of protective structures, a comprehensive study was conducted to evaluate the derailment behavior of trains, the efficacy of protective facilities, and their economic feasibility (Korea Railroad Research Institute, 2024).

The developed DCP structure was designed for application to ballasted tracks of high-speed railways operating at 300 km/h. The design loads were determined using verified FEM simulation models (Song et al., 2019a, 2019b, 2023) and validated techniques derived from full-scale derailment-collision experiments (Bae et al., 2022; Kim et al., 2018). A prototype was fabricated, and its performance was assessed through static load testing (Kim et al., 2024).

Consequently, the derailment containment facilities (DCP) installed at the center of the ballasted track of existing operational lines reduced the impact energy compared to protective walls. Furthermore, the DCP was designed as a single structure, eliminating the need for installation on both sides of the track, thereby ensuring both protective performance and economic efficiency. Additionally, the DCP was designed for quick removal and reinstallation by coupling the steel frame with the concrete sleepers of the ballasted track, facilitating rapid construction and easy maintenance for operational tracks (Kim et al., 2024; Korea Railroad Research Institute, 2024).

Steel frame DCPs for DCP Type 1 are subject to repeated impact loads from successive derailments of wheels at high speeds. Evaluating their impact resistance under cumulative collision loads, dynamic behavior, and durability under repeated loads is crucial because these characteristics cannot be assessed through static load tests alone (Kim et al., 2019; Korea Railroad Research Institute, 2024).

In this study, a new steel grid frame-type DCP was designed and fabricated, distinguishing it from existing DCP Type 1 bridge guardrails, DCP Type 3 protective walls, cast-in-place concrete plinths, and precast concrete panel structures. Drop weight impact tests were introduced to evaluate the dynamic behavior and impact resistance of components such as the steel frame structure, anchors, and concrete sleepers. To analyze damage behavior, 15 drop impact test cases were conducted to estimate impact energy and load for each case, enabling an impact resistance evaluation (Korea Railroad Research Institute, 2024).

## 2 Experiment Overview and Methods

### 2.1 DCP in Railroad Track Gauge Using Grid Frames

As depicted in Fig. 7, the developed grid frame-type DCP is manufactured with a grid frame for use on currently operational ballast tracks. It is installed continuously across the top of PSC concrete sleepers laid on a ballast track. The frame is anchored securely into the sleepers using base plates, mounting blocks, and plastic blocks connected by continuous frame caps. This grid frame configuration not only prevents excessive deviation of a derailed train, but also offers enhanced stability and easier disassembly, which proves advantageous for maintenance on ballast tracks. The dimensions of one grid frame panel are 1775 mm in length, 500 mm in width, and 125 mm in height. The design offers secure continuous placement using three H25 anchors spaced at regular intervals (625 × 3=1875 mm) on the railway ballasted track sleepers (Kim et al., 2024; Korea Railroad Research Institute, 2024).

### 2.2 Experiment Method

The drop weight tower used in this experiment is capable of handling a falling mass ranging from 0.4 to 0.7 tons, with a maximum drop height of 5 to 6 m, thereby imparting a potential energy between 25 to 35 kJ, as shown in Fig. 8. Table 1 details the specifications of the falling mass, which has a total mass of 712 kg. This setup utilizes the principle of gravity to convert potential energy into kinetic energy to strike the sample. In this test, the collision energy is calculated based on the mass and height of the falling body. Quantitative parameters such as acceleration, velocity, displacement, and impact load are measured using accelerometers and high-speed cameras (Kim et al., 2019; Korea Railroad Research Institute, 2024).

The collision behavior was monitored using two high-speed cameras positioned at the front and side of the specimen, recording at a rate of 1000 frames per second (Fig. 9). An acceleration sensor with a 2000*g* capacity was employed to measure the impact load. This sensor recorded data at a high sampling rate of 20,000 Hz (1/20,000 s) to accurately capture the sensor's rapid periodic response. The method for post-processing the impact load data may vary based on the stiffness of the

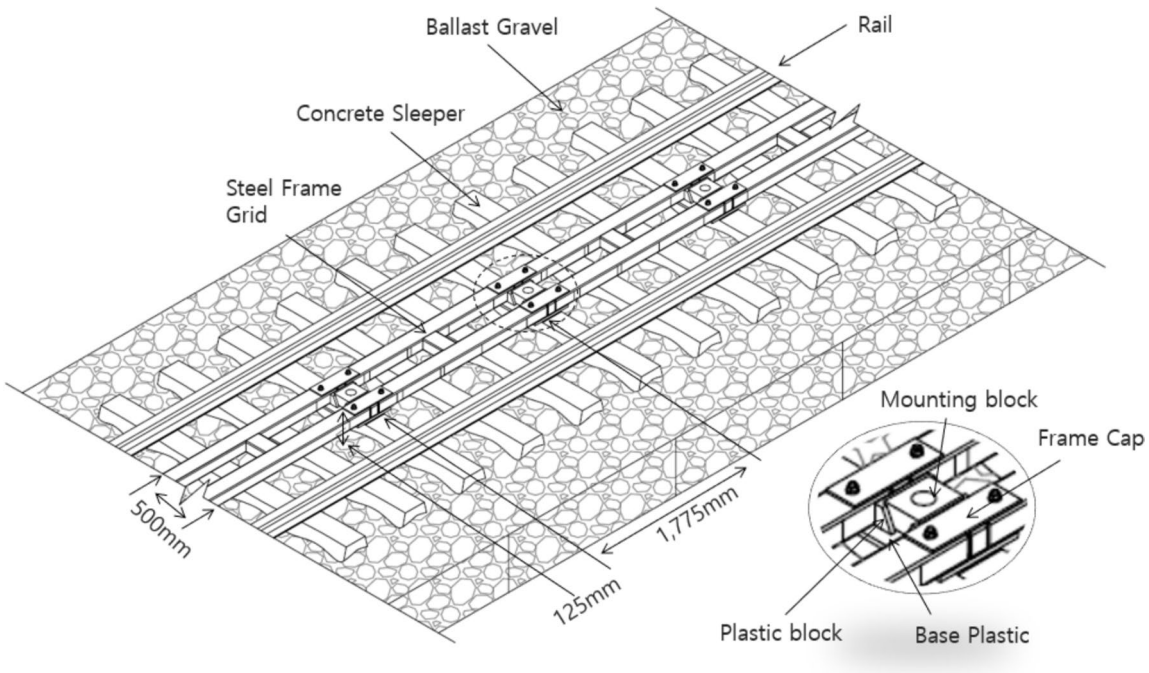


**Fig. 7** Grid frame-type DCP installed on ballast track

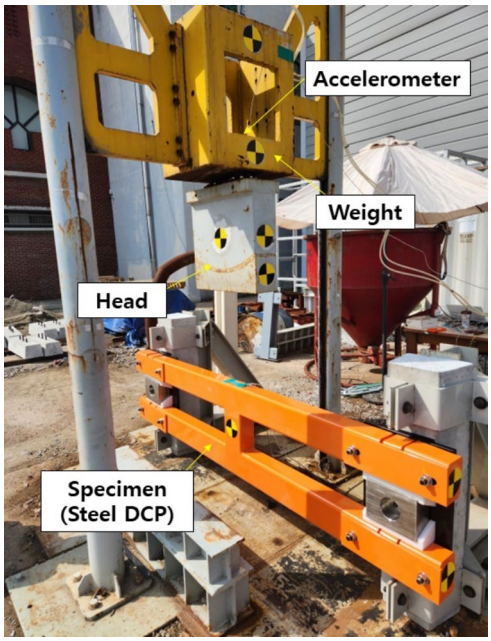


**Fig. 8** View of the drop weight tower and specimens (Korea Railroad Research Institute, 2024)

**Table 1** Falling mass specifications

| Classification | Mass (kg) |
|---|---|
| Weight | 430 |
| Junction | 8 |
| Head | 274 |
| Total | 712 |

specimen and the impact velocity; typically, analysis involves the CFC60 filter, a standard used in full-scale vehicle crash testing for road safety evaluations according to European ISO 6487 (International organization for Standardization, 2000) and American SAE J211 standards (Society of automotive engineers, 2003). In this study, the stresses in the DCP frame, anchor, and sleeper, typically measured during static load testing (Kim et al., 2024), were not recorded. Additionally, the stress in the steel rebar was also not measured.

Wheel derailment occurs when a wheel rotating in contact with the rail deviates laterally from the track. This transverse derailment involves either a point or line contact on the side of the DCP cross-section, where part of the wheel's inner area either touches the surface or forms a specific angle. The points of contact occur in the shape of an arc (Fig. 10a). To simulate this during the test, the head of the falling mass was designed to mimic an impact with a rectangular target, representing the DCP (Fig. 10b). The collision target, the DCP, experiences lateral forces on its side (height 125 mm) as a result of the derailed wheel.

For the purpose of this test, the load application point (contact surface) of the DCP specimen was oriented vertically in line with gravity and securely fastened (Fig. 11). However, the initial condition, where the gravitational force acts downward due to the self-weight of the DCP specimen anchor connected to the sleeper, differs from the real-world scenario.

In actual ballast tracks, the track panel experiences lateral finite stiffness—resistance to lateral motion due to the ballasts—which leads to viscoelastic deformation. Under the conditions of the drop weight impact test, the sides of the sleepers are supported by the ground, which possesses significantly greater stiffness

(a) Impact Head Shape (b) High-speed Camera (c) Accelerometer

**Fig. 9** Drop weight tower setup with specimens (Korea Railroad Research Institute, 2024)

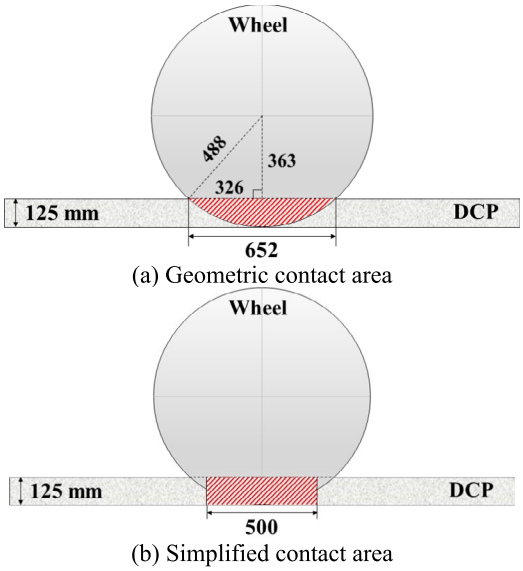


**Fig. 10** Contact area between the DCP and wheel

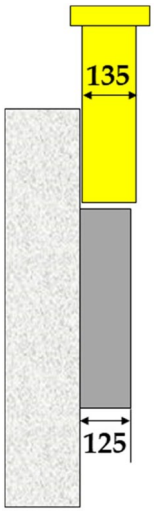


**Fig. 11** Schematic of impact conditions between side of DCP specimen and drop weight

compared to ballast tracks, resulting in relatively minimal lateral deformation of the track panel.

For the test, a fixing jig was fabricated and securely attached (Fig. 12) to prevent the DCP specimen (connected to the sleeper) from toppling when impacted by the mass striking the DCP's side components. The PSC sleepers, utilized in high-speed rail systems where DCPs are installed, are 2600 mm in length. Due to specific test requirements, it was necessary to remove some sections of the sleeper, including those around the anchor and the areas influenced by the DCP. As a result, the sleepers were trimmed, retaining only a central segment of

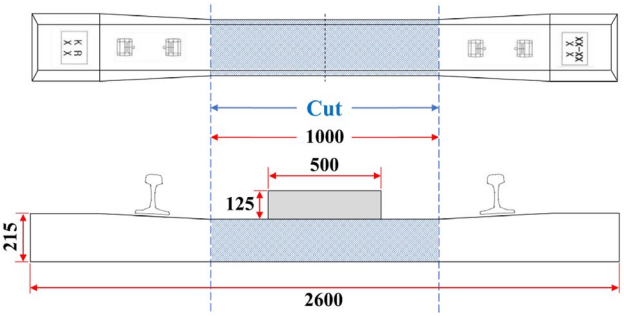


**Fig. 12** Setup of the fixing jig for the PSC sleeper and DCP

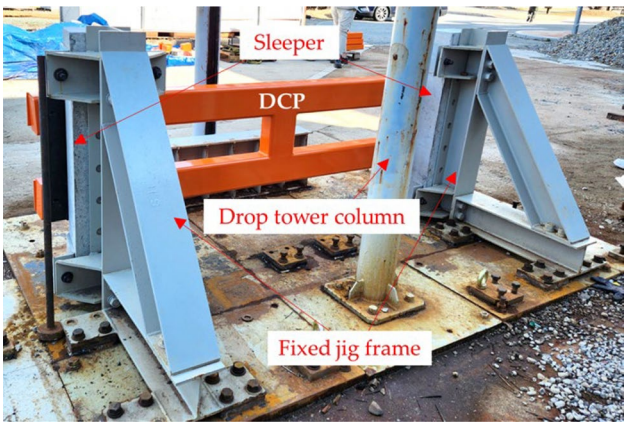


**Fig. 13** Cutting position of PSC sleeper for drop impact tests

1000 mm where the DCP is anchored, as illustrated in Fig. 13 to prevent the DCP specimen (connected to the sleeper) from toppling when impacted by the mass striking the DCP's side components.

The experiment features two primary impact scenarios involving the falling mass and the DCP: 'DCP center collision loading case' and 'DCP anchor collision loading case'. The design of the anchor collision scenario accounted for potential interference between the column of the drop weight tower and the fixing jig. Subsequently, the DCP was positioned and secured using the pre-installed anchors in the sleeper.

Figure 14 illustrates the setup of sleepers and DCP under various impact testing conditions. In the drop weight impact test, after applying the initial target impact energy (approximately 3.5 kJ from a drop height of 0.5 m), the drop height might be increased or additional energy applied depending on the test outcomes.

In this experiment, two identical specimens for each drop impact condition were tested, totaling four specimens. Three buried anchors were pre-installed on each sleeper to secure both the DCP and the PSC sleeper. The sleeper was then anchored to the ground of the

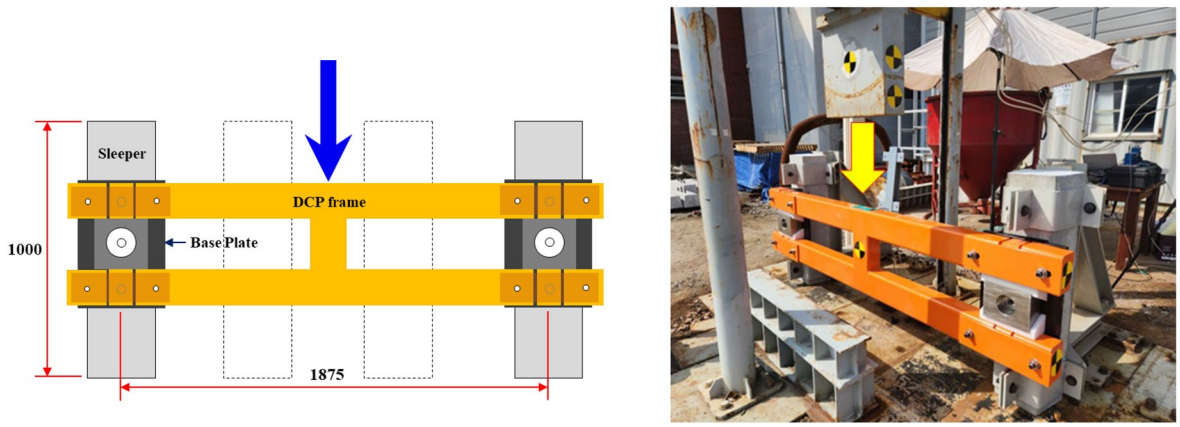


(a) Central Impact Loading

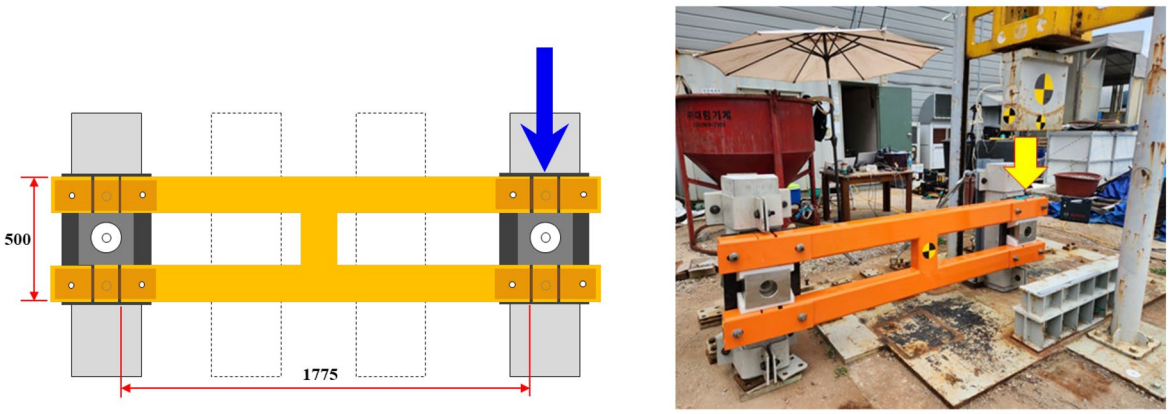


(b) Anchor Impact Loading

**Fig. 14** Schematic and image of impact loading conditions

drop tower, and the base plate was connected to two of the sleeper's anchors, excluding the central anchor. The anchors (four units; inner anchors of both base plates) were aligned with the holes in the DCP frame. The fixings were connected to the sleeper's central anchor (one unit), and the DCP frame was connected to the four inner anchors of the base plate. In a standard setup, two DCP frames would be installed on one base plate; however, for this drop weight impact test, only one DCP frame was installed per base plate. Consequently, the other side of the base plate, not connected to a DCP frame (four units; external anchors), was left as is.

### 2.3 Load Impact Energy

A simulation model, as illustrated in Fig. 15, validated through full-scale railway vehicle derailment-collision experiments (Song et al., 2019b, 2023), was used. This model simulated a scenario involving a KTX train, composed of three cars (power car-motorized car-trailer), derailing while traveling at a speed of 300 km/h on a track with a curve radius of 3500 m (Kim et al., 2020). The model calculated the maximum internal energy per 1-panel (2280 mm long) of DCP colliding with a wheel during a derailment (Table 2). Depending on the situation, a single panel might impact only one wheel of the derailed train, or several wheels might collide with it. A maximum single impact energy of 3.28 kJ (average 0.62 kJ) was derived, with a maximum cumulative impact energy of 5.57 kJ from four impacts. These figures informed the determination of a single drop weight impact test crash energy of 3.5 kJ.

## 3 Experiment Results and Analysis

### 3.1 Experiment Cases

Table 3 presents the drop weight impact test scenarios for the steel frame DCP specimen employed on ballast tracks. Each of the four DCPs was subjected to an

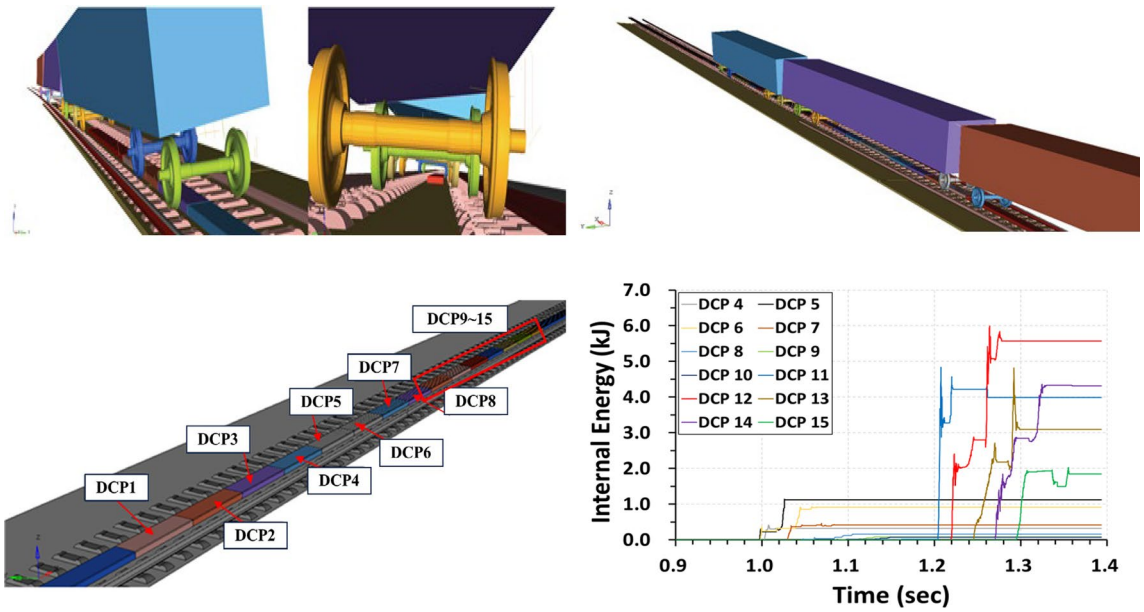


**Fig. 15** High-speed train derailment simulation (Song et al., 2019b, 2023)

**Table 2** Energy metrics of DCP panels

| DCP no. | Max. internal energy per a wheel (kJ) | Cumulative internal energy(kJ) |
|---|---|---|
| DCP 4 | 0.31 (1st/2) | 0.32 |
| DCP 5 | 0.90 (2nd/2) | 1.12 |
| DCP 6 | 0.53 (3rd/5) | 0.91 |
| DCP 7 | 0.37 (1st/3) | 0.42 |
| DCP 8 | 0.05 (4th/5) | 0.16 |
| DCP 9 | 0.04 (2nd/3) | 0.08 |
| DCP 10 | 0.03 (5th/5) | 0.08 |
| DCP 11 | 3.28 (1st/2) | 4.30 |
| DCP 12 | 2.28 (3rd/4) | 5.57 |
| DCP 13 | 2.18 (1st/2) | 3.09 |
| DCP 14 | 2.84 (1st/2) | 4.31 |
| DCP 15 | 1.85 (1st/1) | 1.85 |

**Table 3** Overview of test case configurations

| Specimen no. | Case no. | Impact loading location | Impact energy (kJ) | |
|---|---|---|---|---|
| | | | Impact energy /each event | Accumulated energy |
| #1 | 1 | DCP frame center | 3.5 | 3.5 |
| | 2 | | 3.5 | 7.0 |
| | 3 | | 3.5 | 10.5 |
| #2 | 4 | DCP frame center | 3.5 | 3.5 |
| | 5 | | 3.5 | 7.0 |
| | 6 | | 3.5 | 10.5 |
| | 7 | | 3.5 | 14.0 |
| | 8 | | 3.5 | 17.5 |
| | 9 | | 3.5 | 21.0 |
| #3 | 10 | Connection anchor part | 3.5 | 3.5 |
| | 11 | | 3.5 | 7.0 |
| | 12 | | 3.5 | 10.5 |
| #4 | 13 | Connection anchor part | 3.5 | 3.5 |
| | 14 | | 3.5 | 7.0 |
| | 15 | | 3.5 | 10.5 |

identical drop height (applied impact energy) of 0.5 m, equivalent to 3.5 kJ. The same specimens underwent cumulative collision energies of at least 10.5 kJ on three or more occasions.

## 3.2 Analysis of Main Results

### *3.2.1 Failure Mode according to Impact Condition (Loading Position)*

In the impact scenarios for the central region of the DCP frame (Cases 1–9), as depicted in Fig. 16, the load is distributed between the two sleepers on either side. However, the load primarily affects the inner anchors of the base plate (the four inner anchors out of the total eight on both base plates) that are connected to the loaded DCP frame (1 panel). The transfer of load to the outer anchors, which connect to the other DCP frame, is minimal. After six cumulative impacts totaling 21.0 kJ

(each 3.5 kJ as in Case 9), a notable step has formed between the inner and outer anchors of the base plate (Fig. 16). This discrepancy has led to shear and bearing actions, causing bearing damage to the inner anchor of the base plate as illustrated in Fig. 17.

In the DCP connection anchor impact scenarios (Cases 10–15), as illustrated in Fig. 18, the load is distributed across all four anchors (both internal and external) of a single base plate; however, it is focused on just one sleeper. The initial collision of the falling


**Fig. 16** Specimen appearance post-impact (Case 9)

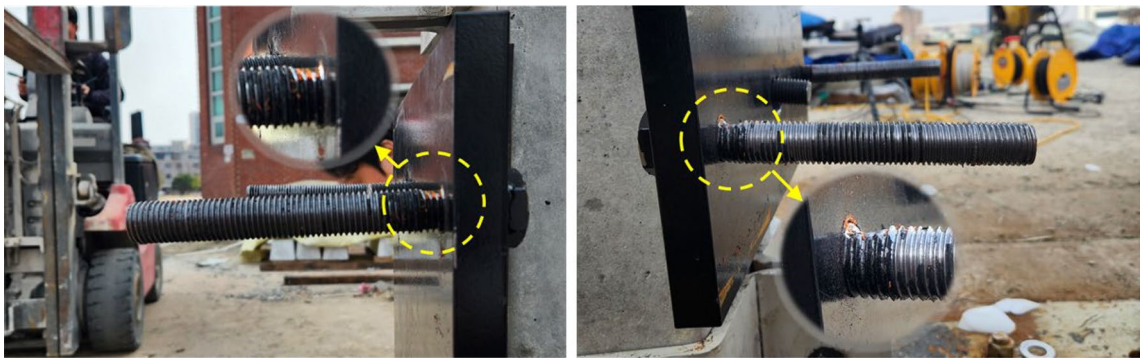

**Fig. 17** Damage to the base plate's inner anchor (Case 9)


**Fig. 18** State of the specimen after drop impact and the geometric conditions of the connection base plate (Case 15)

mass with the lateral side of the base plate results in the majority of the load being exerted on the sleeper and the buried anchors that connect the base plate to the sleeper rather than on the anchors of the base plate itself. After three cumulative impacts totaling 10.5 kJ (each 3.5 kJ as in Case 15), the geometry indicates that the falling mass first impacts the side of the base plate, as shown in Fig. 17. This has led to a splitting failure along the longitudinal axis of the sleeper, following the trajectory of the buried anchors, as shown in Fig. 19.

Figure 19 displays a typical crack pattern observed under extreme loading conditions. When the maximum load capacity was reached, cracks formed along the edge of the concrete at the tension end, corresponding to the bending moment induced by the DCP anchor (SD 400) fixture on the concrete sleeper. The damage pattern reveals that when the wheel impacts the DCP and the force is transmitted through the baseplate to the DCP anchor, substantial shear stress is generated in the concrete sleeper in the perpendicular direction, necessitating a design that can accommodate such stress. There are three primary failure modes experienced by anchors under shear forces: steel failure, concrete failure, and concrete pry-out failure (ACI Committee318, 2014). In situations where the shear force acts perpendicular to the edge of the concrete, as observed in this experiment, the structure is more prone to concrete failure than to anchor failure. The SD400 anchors did not fail under extreme loading, and brittle failure of the concrete occurred after reaching the ultimate load.

#### *3.2.2 Impact Load Patterns According to Impact Position*

Figure 20 illustrates the impact load (filtered using CFC60) exerted on the DCP, calculated by multiplying the acceleration recorded by the accelerometer attached to the falling mass by the mass of the falling object. During a single collision, the load waveform at the point of impact is consistent across both the central and anchor regions; however, in the anchor impact condition, the impact duration was shorter, indicative of stiffer behavior. Over 2 to 3 collisions, the impact load waveform under the central impact condition remains similar, reflecting the shear and bearing resistance of the anchor bolts. Conversely, under the anchor impact condition, the impact duration was longer, and the load magnitude was smaller, corresponding to the cracking and fracturing of the concrete sleeper.

#### *3.2.3 Impact Load and Displacement*

Figure 21 displays the estimated impact load and the vertical displacement of the falling mass's impact head under the center impact condition of the DCP frame (Cases 4–9). During the initial collision (Case 4), the load waveform showed some slippage due to the clearance between the inner anchor of the base plate and the hole in the DCP frame. In subsequent tests assessing the anchoring bolt's stress condition (Cases 6–9), the waveform demonstrated resistance to repetitive impact loads, maintaining a consistent pattern while enduring significant deformation or damage (impact loads approximately 219–285 kN, closely aligning with static load test results (Song et al.,


**Fig. 19** Damage to sleeper and buried anchors post-impact (Cases 12 and 15)

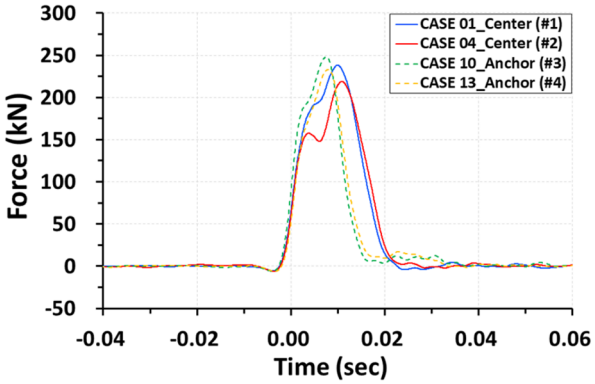


(a) 1st impact (3.5 kJ).

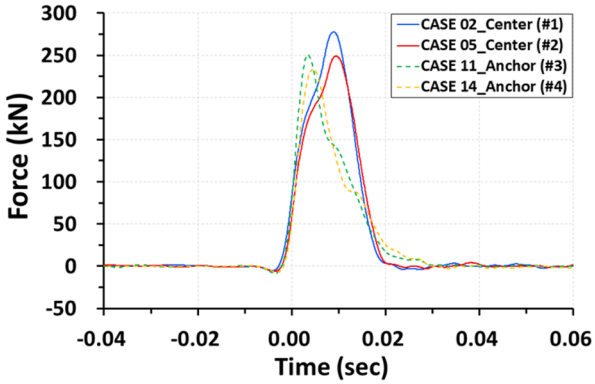


(b) 2nd impact (7.0 kJ; cumulative energy).

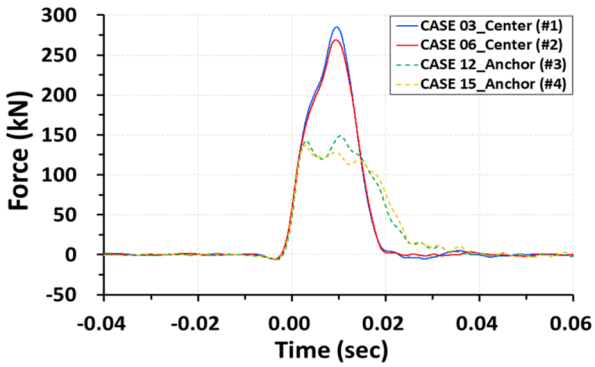


(c) 3rd impact (10.5 kJ; cumulative energy).

**Fig. 20** Impact force estimates by location (from accelerometer data)

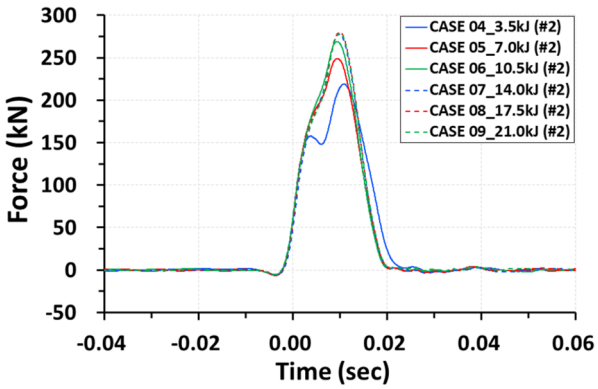


(a) Impact force of the DCP frame center

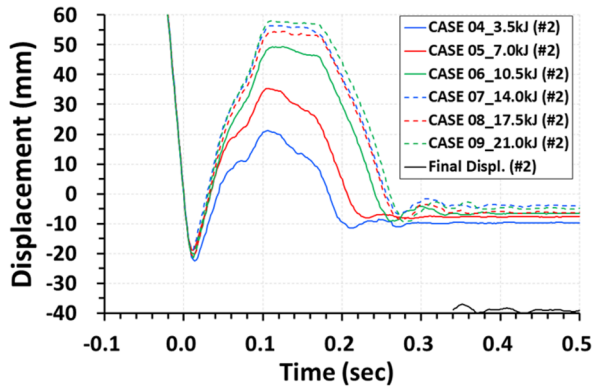


(b) Displacement of the mass head

**Fig. 21** Impact force and displacement of the falling mass head at the DCP center

2019b) in the range of 210–290 kN). The displacement of the impact head was determined through high-speed camera tracking analysis. The observed rebound resulted from the elastic rebound of the base plate anchor bolts, which bear the primary load following the collision between the impact part and the DCP. The extent of the rebound is generally proportional to the magnitude of the impact load. The final cumulative residual displacement at the center of the DCP frame, after six impacts totaling 21.0 kJ, was approximately 39 mm.

Figure 22 depicts the estimated impact load and vertical displacement of the falling mass impactor (head) under the DCP connection anchor impact condition (Cases 10–15). At the initial impact (Cases 10 and 13), the collision load waveform displayed a pattern akin to that observed in the central impact condition. The crash anchors underwent some plastic displacement but withstood the impact without significant damage [crash loads approximately 233–250 kN, aligning with static load test results of 210–250 kN (Song et al., 2019b)]. During two cumulative collisions (Cases 11 and 14), cracks formed along the longitudinal axis of the sleeper, following the buried anchors. This led to an increased impact load duration due to the associated increase in deformation. In the three cumulative collisions (Cases 12 and 15), longitudinal splitting failures of the sleeper occurred, extending the duration of crash load action and significantly reducing the crash load magnitude [137 to 149 kN, below the designed crash load of 166 kN (Song et al., 2019b)]. Specimens #3 and #4 exhibited remarkably similar results under these identical impact conditions.

Data from the falling mass impact head (Fig. 18b) indicate that the extent of rebound due to the resistance of the concrete buried anchors under dominant loading is less compared to the impact condition at the center of the DCP frame, while the residual (plastic) displacement is significantly greater. The final cumulative residual displacement of the connection anchor, after three impacts totaling 10.5 kJ, was approximately 49 mm. The outcomes of these experiments are detailed and summarized in Table 4.

## 4 Conclusion

In this study, the dynamic load-bearing characteristics of the steel grid frame-type DCP combination structure, designed and manufactured as DCP Type 1 to enable rapid assembly and maintenance on ballasted tracks in operation, were evaluated. Previous studies examined the load-bearing capacity against design loads through static load tests; however, it is crucial to assess the collision performance of the assembled DCP structure under dynamic impact loads from continuously colliding wheels. To address this, this study newly proposed a drop weight test for the DCP combination structure and analyzed its behavior when impact energy was cumulatively applied to major impact locations. The testing and analytical methodologies proposed in this study enable the identification of dynamic behavioral characteristics of structures subjected to similar collisions and repeated loads caused by derailments.

A drop weight test was conducted on the steel grid frame-type DCP combination structure. The test simulated situations where wheels derailed from the rail continuously collided with the steel grid frame-type DCP, and the dynamic behavior of the DCP components under cumulative impact energy was analyzed. The analysis results are as follows:

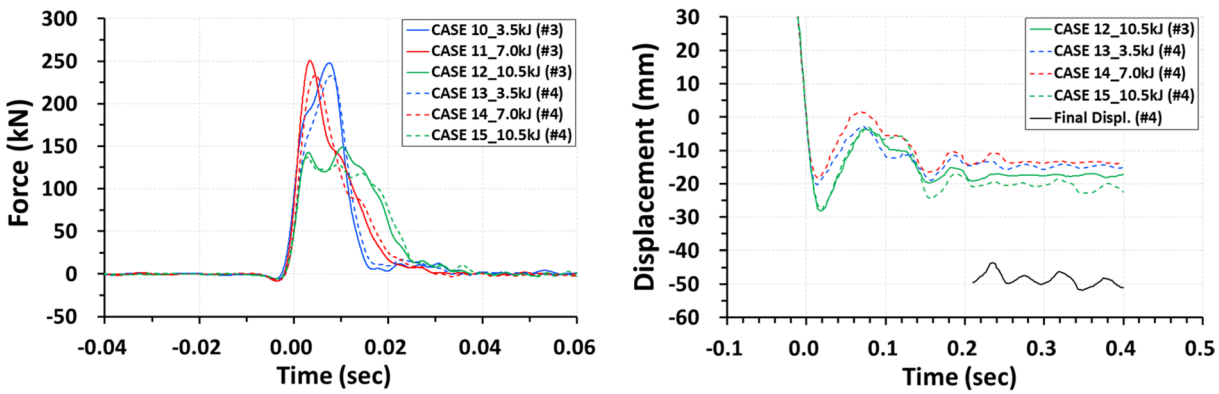


(a) Impact force of the connection anchor part (b) Displacement of the mass head

**Fig. 22** Impact force and displacement at the connection anchor

**Table 4** Summary of experimental results

| Case | Test specimen | Impact energy (kJ) | Impact load[1] (kN) | Residual displacement of test specimen[2] (mm) | | | Note |
|---|---|---|---|---|---|---|---|
| | | | | Center of DCP (dynamic cone penetrometer) (vertical) | Outer anchor part (vertical) | Outer anchor part (horizontal) | |
| 1 | #1 Central collision | 3.5 | 238.47 | 1.90 | 1.70 | 1.54 | ·Resisted without significant deformation or damage. |
| 2 | | 3.5 (7.0) | 277.72 | 8.74 (10.63) | 1.57 (3.27) | 4.53 (6.07) | ·Resisted without significant deformation or damage. |
| 3 | | 3.5 (10.5) | 284.96 | 4.90 (15.53) | 0.94 (4.21) | 2.74 (8.81) | ·Resisted without significant deformation or damage. |
| 4 | #2 Central collision | 3.5 | 219.05 | 9.74 | 0.01 | 0.03 | ·Resisted without significant deformation or damage. |
| 5 | | 3.5 (7.0) | 248.96 | 7.74 (17.49) | 0.12 (0.13) | 1.46 (1.49) | ·Resisted without significant deformation or damage. |
| 6 | | 3.5 (10.5) | 268.98 | 6.63 (24.11) | 0.16 (0.29) | 0.01 (1.49) | ·Resisted without significant deformation or damage. |
| 7 | | 3.5 (14.0) | 277.46 | 3.99 (28.10) | 1.48 (1.78) | 0.08 (1.58) | ·Resisted without significant deformation or damage. |
| 8 | | 3.5 (17.5) | 279.84 | 6.24 (34.34) | 1.69 (3.47) | 1.43 (3.01) | ·Resisted without significant deformation or damage. |
| 9 | | 3.5 (21.0) | 278.88 | 4.85 (39.19) | 1.82 (5.29) | 0.06 (3.07) | ·Resisted without significant deformation or damage.<br>·Damage to the inner anchor of the base plate due to pressure. |
| **Case** | **Test specimen** | **Impact energy (kJ)** | **Impact Load[1] (kN)** | **Residual displacement of test specimen[2] (mm)** | | | **Note** |
| | | | | **Top surface of anchor (vertical)** | **Outer anchor part (vertical)** | **Outer anchor part (horizontal)** | |
| 10 | #3 Anchor collision | 3.5 | 248.05 | – | – | – | ·The collision caused plastic deformation in the anchor part, but it resisted without significant damage. |
| 11 | | 3.5 (7.0) | 250.50 | – | – | – | ·Cracks developed along the buried anchor in the direction of the pile length. |
| 12 | | 3.5 (10.5) | 148.61 | 17.49 | 14.09 | 5.75 | ·Fracture occurred along the buried anchor in the direction of the pile length. |
| 13 | #4 Anchor collision | 3.5 | 233.03 | 14.84 | 13.86 | 8.79 | ·The collision caused plastic deformation in the anchor part, but it resisted without significant damage. |
| 14 | | 3.5 (7.0) | 233.30 | 13.61 (28.46) | 8.78 (22.63) | 5.60 (14.39) | ·Cracks developed along the buried anchor in the direction of the pile length. |
| 15 | | 3.5 (10.5) | 136.77 | 20.84 (49.29) | 16.54 (39.17) | 14.76 (29.15) | ·Fracture occurred along the buried anchor in the direction of the pile length. |

**Table 4** (continued)

[1] Acceleration sensor data considering the total mass of the falling weight (with CFC60 filter applied).

[2] Deriving displacement at specific points on the test specimen using high-speed camera image tracking.

(1) When the wheels of a derailed train collide with the DCP frame, the primary load acts on the base plate anchors and is resisted by the shear and bearing strength of the anchor bolts. Despite significant cumulative energy (21.0 kJ; six consecutive impacts), the impact load and displacement levels sufficiently ensured the derailment containment performance. For repetitive impact loads (10.5–21.0 kJ; 3–6 impacts) in a bearing state, the collision load absorbed by the DCP main frame was calculated to average 276.29 kN. The vertical displacement at the collision location was analyzed to be minimal, with an average of 5.43 mm, even under repeated impacts.

(2) When the wheels of a derailed train collide with the DCP connection anchor, the primary load acts on the sleeper's embedded anchors and is resisted by the concrete strength of the sleeper. As the DCP frame covers a significantly larger area (approximately 75%) than the connection anchor, the probability of a derailed wheel colliding directly with the anchor is relatively low. However, if repetitive collisions occur on the anchor, there is a high likelihood of damage severe enough to require sleeper replacement. For repetitive impact loads (3.57–7.0 kJ; 1–2 impacts), the collision load absorbed by the DCP connection anchor was calculated to average 241.22 kN. The vertical displacement at the collision location was found to be 14.23 mm on average, which is 2.62 times (162%) larger compared to collisions on the DCP frame. Additionally, it was approximately 13% lower than the collision load that the DCP frame can accommodate. However, it should be noted that the results were evaluated under highly conservative conditions due to the constraints of this drop weight test, such as the restriction of lateral displacement in the track structure, which imposes severe conditions on the anchor side. Therefore, the results may differ significantly from actual field conditions.

(3) When a derailed wheel directly collides with the side of the base plate, the embedded anchors in the sleeper become relatively more vulnerable compared to other areas. Adjusting the dimensions of the base plate (reducing the width from 500 mm to 480 mm) to direct the collision toward the DCP frame is imperative for minimizing the impact damage on the concrete sleeper. This adjustment allows the base plate anchor bolts, which can accommodate greater collision loads, to exhibit dominant behavior.

(4) In this study, the newly proposed drop weight test for the DCP combination structure enables the identification of the dynamic behavior characteristics of structures subjected to repeated loads from derailed wheels colliding with the DCP. This approach allows for evaluating the durability and protective performance of similar structures, including the DCP, in the event of a vehicle derailment and subsequent collisions in the future.

(5) Dynamic analysis of DCP collisions following vehicle impacts has been conducted in previous studies to estimate the impact energy applied during the tests. In the future, finite element analysis must be performed to investigate the detailed behavior of each component of the steel grid frame-type DCP after derailment and wheel collisions. It is also necessary to compare and analyze the results with experimental findings.

**Acknowledgements**
This research received funding from the Railway Technology Research Program, supported by Grant RS-2021-KA163289 from the Ministry of Land, Infrastructure, and Transport of the Korean government.

**Author contributions**
YSK planned this paper, developed the steel-frame DCP, and analyzed the experimental results. HUB tested the experimental results and the numerical results. THK, CSB, NHL, CYL, WJH designed DCP specimens. All authors read and approved the final manuscript.

**Funding**
This research received funding from the Railway Technology Research Program, supported by Grant RS-2021-KA163289 from the Ministry of Land, Infrastructure, and Transport of the Korean government.

**Availability of data and materials**
The research data used to support the finding of this study are described and included in the article. Furthermore, some of the data used in this study are also supported by providing references as described in the article.

## Declarations

**Competing interests**
The author declares no competing interests.

**Author details**
[1]Advanced Railroad Civil Engineering Division, Korea Railroad Research Institute, 176, Cheoldobangmulgwan-ro, Uiwang-si, Gyeonggi-do 16105, Korea. [2]Director of Research Institute, Road Kinematics co., Ltd., Baekseokgongdan 1-ro, Seobuk-gu, Cheonan-si, Chungcheongnam-do 31094, Korea. [3]Department of Civil Engineering, Chungnam National University, 99 Daehak-ro, Yusung-Gu, Daejeon 34134, Korea. [4]Technology Research Institute, ESCO RTS

Co., Ltd., 52, Maehyang-gil, Seoun-myeon, Anseong-si, Gyeonggi-do 17608, Korea. [5]Railway Division, ESCO RTS Co.,Ltd., 52, Maehyang-gil, Seoun-myeon, Anseong-si, Gyeonggi-do 17608, Korea.

Received: 15 October 2024 Accepted: 1 February 2025
Published online: 14 May 2025

**References**

ACI Committee 318. (2014). *Building code requirements for reinforced concrete (ACI 318–14) and commentary (ACI 318R-14)*. American Concrete Institute.

American Association of State Highway and Transportation Officials. "AASHTO LRFD Bridge Design Specifications". *SI Units 4th Edition Vol.2, Section 13: Railings, 2007*.

Aviation and Railway Accident Investigation Board. (2023). *Casebook of Aviation and Railway Accidents*

Bae, H.U. (2015). *Advanced design concept of derailment containment provisions using collision simulation after train derailment*. Ph.D. dissertation, Chungnam National University. https://www.riss.kr/link?id=T13851809

Bae, H. U., Kim, K. J., Park, S. Y., Han, J. J., Park, J. C., & Lim, N. H. (2022). Functionality analysis of derailment containment provisions through full-scale testing-I: collision load and change in the center of gravity. *Applied Sciences, 12*(21), 11297. https://doi.org/10.3390/app122111297

Bae, H. U., & Lim, J. H. (2024). Application effectiveness and priority of installation of derailment containment provisions. *The Magazine 2024, Korean Society of Hazard Mitigation, 24*(2), 17–22. in Korean.

Bae, H. U., Moon, J. H., Lim, S. J., Park, J. C., & Lim, N. H. (2019). Full-scale train derailment testing and analysis of post-derailment behavior of casting bogie. *Applied Sciences, 10*(1), 59. https://doi.org/10.3390/app10010059

Bae, H. U., Yun, K. M., & Lim, N. H. (2018a). Containment capacity and estimation of crashworthiness of derailment containment walls against high-speed train. *Proceedings of the Institution of Mechanical Engineers, Part f: Journal of Rail and Rapid Transit., 232*(3), 680–696. https://doi.org/10.1177/0954409716684663

Bae, H. U., Yun, K. M., Moon, J., & Lim, N. H. (2018b). Impact force evaluation of the derailment containment wall for high-speed train through a collision simulation. *Advances in Civil Engineering*. https://doi.org/10.1155/2018/2626905

Booz Allen Hamilton Inc. (2004). *Report on the Findings of: Current Practice and Effectiveness of Derailment Containment Provisions on High-Speed Lines*. Issue 1, Ref: R00673, HSL-Zuid Organisation, Zoetermeer, Netherlands.

FRA. (2011). *FRA guide for preparing accident/incident reports*. U.S. Department of Transportation.

International Organization for Standardization. (2000). *Road vehicles: Measurement techniques in impact tests—Instrumentation*. ISO 6487, International Standard.

Iwnicki, S., Wu, H., & Wilson, N. (2006). *Handbook of railway vehicle dynamics: railway vehicle derailment and prevention*. Taylor and Francis Group. https://doi.org/10.1201/9781420004892

Kim, J. H., Bae, H. U., Kim, J. W., Song, I. H., Lee, C. O., & Lim, N. H. (2018). Post-derailment behavior of casting bogie by full -scale test. *Journal of the Korean Society for Railway., 21*(8), 815–829. https://doi.org/10.7782/JKSR.2018.21.8.815. in Korean.

Kim, N. H., Kang, Y. S., Bae, H. U., Kim, K. J., & Lim, N. H. (2020). Evaluation of impact resistance for derailment containment provision using drop weight test. *Journal of the Korean Society of Hazard Mitigation., 20*(5), 185–194. https://doi.org/10.9798/KOSHAM.2020.20.5.185. in Korean.

Kim, T. H., Kang, Y. S., & Bang, C. S. (2024). Structural performance assessment of derailment containment provision for railway using a grid steel frame. *International Journal of Concrete Structures and Materials, 18*(5), 13. https://doi.org/10.1186/s40069-023-00640-1

Kim, Y. D., Lim, S. J., Bae, H. U., Kim, K. J., Lee, C. O., & Lim, N. H. (2019). Some thought on the estimating of the impact force by an experiment. *Journal of Korean Society for Urban Railway., 7*(2), 205–213. https://doi.org/10.24284/JKOSUR.2019.6.7.2.205. in Korean.

Korea Agency for Infrastructure Technology Advancement (KAIA). (2020). *Research for Development and Design Criteria of Derailment Containment Provisions for Railway Vehicle*. Project No. 19RTRP-B122273-04, Ministry of Land, Infrastructure, and Transport.

Korea Railroad Research Institute. (2024). Steel frame-type falling impact protection facility performance testing service. *Technical Report*, 5–9. (**in Korean**)

Liu, X., Saat, M. R., & Barkan, C. P. L. (2012). Analysis of causes of major train derailment and their effect on accident rates. *Transportation Research Record*. https://doi.org/10.3141/2289-20

Liu, X., Saat, M. R., & Barkan, C. P. L. (2017). Freight-train derailment rates for railroad safety and risk analysis. *Accident Analysis & Prevention*. https://doi.org/10.1016/j.aap.2016.09.012

Massachusetts Board of Railroad Commissioners (1888). "Report of the board of railroad commissioners in relation to the accident on the Boston and Maine railroad (western division)", Near Bradford, January 10, 1888.

Network Rail (NR), Design of bridges (design loading for accommodation and occupation overbridges), *NR/L3/CIV/020, Network Rail Kings Place, London, UK, 2011*.

Railtrack PLC (Safety & Standards Directorate), Recommendations for the Design of bridges, railtrack approved code of practice, *GC/RC5110, Railtrack PLC, London, UK, 2000*.

Society of automotive engineers. (2003). *SAE J211: Instrumentation for impact tests*.

Song, I. H., Kim, J. W., Koo, J. S., Bae, H. U., & Lim, N. H. (2019a). Simplified vehicle modeling technique for design of derailment containment provisions (DCP). *Journal of the Korean Society for Railway, 22*(7), 527–537. https://doi.org/10.7782/JKSR.2019.22.7.527. in Korean.

Song, I. H., Kim, J. W., Koo, J. S., & Lim, N. H. (2019b). Modeling and simulation of collision-causing derailment to design the derailment containment provision using a simplified vehicle model. *Applied Sciences, 10*(1), 118. https://doi.org/10.3390/app10010118

Song, I. H., Koo, J. S., Shim, J. S., Bae, H. U., & Lim, N. H. (2023). Theoretical prediction of impact force acting on derailment containment provisions (DCPs). *Applied Sciences, 13*(6), 3899. https://doi.org/10.3390/app13063899

Wu, X., Chi, M., & Gao, H. (2014). The study of post-derailment dynamic behavior of railway vehicle based on running tests. *Engineering Failure Analysis, 44*, 382–399. https://doi.org/10.1016/j.engfailanal.2014.05.021

## Publisher's Note



**Yun-Suk Kang** Yun-Suk Kang is a Chief Researcher in the Advanced Railroad Civil Engineering Division at the Korea Railroad Research Institute, Uiwang-si, Korea. He received his PhD in structural engineering from Korea University, Seoul, Korea. His research interests include railway track, performance evaluation of railway system as well as the development of new type railway structure.

**Hyun-Ung Bae** Hyun-Ung Bae is a director of research institute in the Road Kinematics co., Ltd., Cheonan-si, Korea. He received his PhD in structural engineering from Chungnam National University, Daejeon, Korea. His research interests include railway track and structural engineering, and collision analysis.

**Tae-Hoon Kim** Tae-Hoon Kim is a Principal Researcher in the Advanced Railroad Civil Engineering Division at the Korea Railroad Research Institute, Uiwang-si, Korea. He received his PhD in structural engineering from Sungkyunkwan University, Seoul, Korea. His research interests include nonlinear analysis and design of concrete structures, constitutive modeling, and seismic performance assessment.

**Choon-Seok Bang** Choon-Seok Bang is a Principal Researcher in the Advanced Railroad Civil Engineering Division at the Korea Railroad Research Institute, Uiwang-si, Korea. He received his PhD with a Structural Model of Concrete at the Korea Railroad Research Institute, Uiwang-si, Korea. He received his PhD with a Structural

Model of Concrete Structures, as well as the Development of New Technologies.

**Nam-Hyung Lim** Nam-Hyung Lim is a Professor of Chungnam National University in the Advanced Railroad Civil Engineering Division at the Daejeon-si, Korea. He received his PhD in structural engineering from Korea University, Seoul, Korea, His research interests include railway track, structural engineering and nonlinear analysis of Continuous Welded Rail Tracks.

**Chan-Young Lee** Chan-Young Lee is a Managing Director in the the Railway Business Department at the ESCORTS.,Ltd , Ansung si, Korea. He received his ME with structural engineering from Incheon National University. His research interests include the design, compositional modeling, and seismic performance evaluation of vibration reduction devices.

**Woo-Jin Han** Woo-Jin Han is a Senior Researcher in the the Railway Business Department at the ESCORTS.,Ltd, Ansung si, Korea. He received his BS with New material engineering from Suwon University. His research interests include the design, compositional modeling, and seismic performance evaluation of vibration reduction devices.